*Journal of* ELECTRICAL ENGINEERING, VOL 72(2021), NO5, 297–305

sciendo

PAPERS

# Estimation of parameters of a sum of sinusoids sampled below the Nyquist rate with frequencies away from the grid

**Igor Djurović**[1,2]

We are witnessing a growing interest in processing signals sampled below the Nyquist rate. The main limitation of current approaches considering estimation of multicomponent sinusoids parameters is the assumption of frequencies on the frequency grid. The sinusoids away from the frequency grid are considered in this paper. The proposed procedure has three stages. In the first two, a rough estimation of signal components is performed while in the third refinement in estimation is achieved in a component-by-component manner. We have tested the developed technique on an extended set of simulation examples showing excellent accuracy. Three scenarios are considered in experiments: missing samples, noisy environment, and non-uniform sampling below the Nyquist rate.

K e y w o r d s: grid frequency, non-uniform sampling, sampling below the Nyquist rate

## 1 Introduction

Estimation of sinusoidal parameters is evergreen in the signal processing community [1–8]. Development of the signal processing field was closely related to sinusoids and such interest is lasting. Recently, the emerging field of compressive sensing signal processing handling the signals sampled below the Nyquist criterion has attracted significant attention of the scientific community [9–11]. Reconstruction of an undersampled and non-uniformly sampled sum of sinusoids has importance in various applications. The most notable application area is radar signal processing [12]. Existing approaches usually treat the sum of undersampled and non-uniformly sampled sinusoids but with frequencies on the discrete Fourier transform (DFT) grid. These signals are sparse in the DFT domain. However, a sum of sinusoids that are away from the grid is not sparse in the DFT domain due to side lobes appearing at all frequency bins. It is a violation of the restricted isometry property common for the compressive sensing framework [13]. However, the sum of sinusoids is always sparse in the continuous-time FT domain. Therefore, the possibility to develop an appropriate estimation algorithm for such signals is investigated. In this research, we developed a three-stage procedure for estimating the sum of sinusoids sampled below the Nyquist rate with off-the-DFT grid frequencies. The first stage is devoted to a rough estimation of signal components, the second stage improves accuracy in amplitude and phase estimation for all components at once. The third stage improves accuracy in the estimation of each signal component separately. The rerun of the third stage is beneficial for improving accuracy in the estimation process. The Aboutanios-Mulgrew algorithm is used in the first and third stages [4]. In the second stage, the amplitudes and phases are re-estimated at once with a common technique forthe compressive sensing of sinusoids [9].

## 2 Signal model

Consider the sum of sinusoids

$$x(n) = \sum_{m=1}^{M} A_m \exp(j\omega_m n + j\varphi_m),\ n \in [1, N]\ , \qquad (1)$$

where $A_i$, $\omega_i$, and $\varphi_i$ are amplitudes, frequencies and phases of signal components respectively. All frequencies are distinct $\omega_i \neq \omega_j$ for $i \neq j$. We assume that instead of $N$ uniformly sampled samples according to the Nyquist criterion we have $K$ randomly sampled samples indexed as $n_k \in [1, N]$, $k \in [1, K]$, $K < N$ and for simplicity assume $n_k < n_{k+1}$:

$$x(n_k) = \sum_{m=1}^{M} A_m \exp(j\omega_m n_k + j\varphi_m), k \in [1, K], n_k < n_{k+1}\ . \qquad (2)$$

The goal is the estimation of signal parameters from observation of $x(n)$. For simplicity reasons it is assumed that number of sinusoids $M$ is known in advance. There are several available algorithms for this purpose [9, 10], with the main obstacle that it is assumed that sinusoidal frequency belongs to the grid. The signal model without this limitation is considered in this paper.

[1] University of Montenegro, Electrical Engineering Department, Cetinjski put bb, 81 000 Podgorica, Montenegro, [2] Montenegrin Academy of Sciences and Arts, Rista Stijovića 5, 81000 Podgorica, Montenegro, igordj@ucg.ac.me

https://doi.org/10.2478/jee-2021-0042, Print (till 2015) ISSN 1335-3632, On-line ISSN 1339-309X

## 3 Algorithm

The algorithm is organized into three stages. In the first stage, components with estimated parameters are peeled off with subsequent estimation of weaker sinusoids. The second stage considers the refinement of amplitude and phase estimates. The third stage is similar to the initial stage but now the strongest components are also estimated with removed weaker ones estimated from the previous two stages. The main issue in the proposed approach is the accurate estimate of signal frequency. For this purpose, we have employed the Aboutanios-Mulgrew algorithm in the first and third algorithm stages as a simple and effective solution for this problem. This interpolator achieves a trade-off between complexity and accuracy among many recently developed counterparts. Describe now three algorithm stages in detail.

### *3.1 First stage – initial parameter estimation*

In this stage, a search for the DFT maxima position is performed. The position of the maxima is then refined as an estimator of the component frequency using the Aboutanios-Mulgrew algorithm [4]. The dominant component is removed and estimation of the second component is performed. The procedure is repeated for each component in the mixture. However, the entire procedure brings inaccuracy in the process. The strongest components are affected by weaker ones that are not removed from the mixture while inaccuracy in estimation of the strongest components has an impact on the estimation of the weaker ones. This issue has been studied in [11] where it is shown that the residual error caused by uncompensated parts of signal components can be modeled as a (Gaussian) noise with variance proportional to the percentage of missing samples. This implies the development of the other algorithm stages described subsequently.

The algorithm scheme for the first stage is summarized below.

- Set $x^{(0)}(n_k) = x(n_k),\ k \in [1, K]$.

For $m = 1 : M$

Calculate

$$X^{(m)}(k) = \frac{1}{K}\sum_{k=1}^{K} x^{(m-1)}(n_k)\exp\left(-j\frac{2\pi k}{N}n_k\right). \quad (3)$$

This form of the DFT is the counterpart of the L-DFT proposed in [14] for estimation of the DFT of the noisy signal corrupted by impulsive noise. The single notable difference is that the positions of uncorrupted samples are known in the compressive sensing framework.

- Estimate frequency of the $m$-th component based on the position of the DFT maxima.

$$\hat{\omega}^{(m)} = \frac{2\pi}{N}\hat{k} = \frac{2\pi}{N}\arg\max_k |X^{(m)}(k)|\,. \quad (4)$$

However, this is a rough estimate of the DFT corresponding to the frequency grid. The accuracy of this estimate is weak so we have to employ an efficient procedure to refine it. The oversampling of the DFT grid is demanding. Therefore, employing efficient DFT interpolators is common in the field. Due to advantages, the Aboutanios-Mulgrew algorithm is clear choice for this purpose [4]. Note that it is already applied to the impulsive noise environment [6, 7]. It can be described as follows.

- Set $\delta = 0$, and $q = 1 : Q$

$$\delta = \delta + \frac{1}{2}\frac{|X^{(m)}(\hat{k}+\delta+\frac{1}{2})| - |X^{(m)}(\hat{k}+\delta-\frac{1}{2})|}{|X^{(m)}(\hat{k}+\delta+\frac{1}{2})| + |X^{(m)}(\hat{k}+\delta-\frac{1}{2})|}\,. \quad (5)$$

Hereafter, we are freely using computer programming notation with a result from the right-hand updating the left-hand side of the equation.

Note, that the required number of iterations for fully sampled signal and Gaussian environment is only $Q = 2$. However, for impulsive noise environment or the considered case of missing samples it should be larger with the appropriate value in a range $Q \in [5, 10]$ (see [6]).

- Frequency estimate is updated as

$$\hat{\omega}^{(m)} = \hat{\omega}^{(m)} + \frac{2\pi}{N}\delta\,. \quad (6)$$

Now component with this frequency should be eliminated from mixture. It is performed as described below.

- Amplitude and phase estimates of the component are obtained as

$$Z = \frac{1}{K}\sum_{k=1}^{K} x^{(m-1)}(n_k)\exp\big(-j\hat{\omega}^{(m)}n_k\big), \quad (7)$$

$$\hat{A}_m = |Z|\,, \quad \hat{\varphi}_m = \measuredangle Z\,. \quad (8,9)$$

- Estimated component is removed from the mixture:

$$\begin{aligned} x^{(m)}(n_k) &= x^{(m-1)}(n_k) - Z\exp\big(j\hat{\omega}^{(m)}n_k\big) \\ &= x^{(m-1)}(n_k) - \frac{\exp\big(j\hat{\omega}^{(m)}n_k\big)}{K}\times \\ &\quad \times\sum_{k=1}^{K} x^{(m-1)}(n_k)\exp\big(-j\hat{\omega}^{(m)}n_k\big). \end{aligned} \quad (10)$$

However, the estimates (6), (8), (9), are only rough due to influence of other components. Therefore, we can proceed with the other algorithm stages.

### *3.2 Second stage*

After the first rough stage, we can assume that we have a relatively accurate set of frequency estimates but with potential for some percentage of outliers. In this stage, amplitude and phases are re-estimated using the classical least-squares procedure so it is not possible to remove outliers from the first stage since they are associated with wrong frequency estimates. In this procedure amplitudes and phases of all components from the previous stage are refined at once. The procedure is described below.

Refinement of the amplitude and phase estimates can be written by the following equation:

$$\boldsymbol{c} = \boldsymbol{A}^{-1}\boldsymbol{b}\,, \tag{11}$$

where elements of the vector column $\boldsymbol{b}$ are

$$b_m = \sum_{k=1}^{K} x(n_k)\exp\bigl(-j\hat{\omega}^{(m)}n_k\bigr)\,, \tag{12}$$

while elements of matrix $\boldsymbol{A}$ are

$$a_{ml} = \sum_{k=1}^{K}\exp\bigl(-j[\hat{\omega}^{(m)} - \hat{\omega}^{(l)}]n_k\bigr). \tag{13}$$

Amplitude and phase estimates are obtained from vector column $\boldsymbol{c}$ as

$$\hat{A}'_m = |c_m|\,, \quad \hat{\varphi}'_m = \measuredangle c_m\,. \tag{14}$$

### *3.3 Third stage – component-by-component estimation refinement*

Here, the procedure is performed similarly as in the initial stage but with a notable difference that the strongest component is estimated with removed remaining ones. Other components are removed using estimates obtained in the previous stages. Then, each component is re-estimated with other components removed. This procedure reduces the number of outliers in the estimation of the signal frequencies. The outliers in the first two stages most commonly appear for weaker components, especially if they are close in the frequency domain to stronger components. However, when other components are estimated more precisely it is possible to remove them more accurately and to make an easier estimation of the weaker neighbors.

Inputs for the third stage are set of frequency estimates $\hat{\omega}^{(m)\prime\prime} = \hat{\omega}^{(m)}$ and amplitude and phase estimates $\hat{A}''_m = \hat{A}'_m$ and $\hat{\varphi}''_m = \hat{\varphi}'_m$ from the previous stages.

- For $m = 1 : M$

  Estimate of the $m$-th sinusoid as

$$\hat{x}_m(n_k) = x(n_k) - \sum_{\substack{l=1\\ l\neq m}}^{M}\hat{A}''_l\exp\bigl(j\hat{\omega}^{(l)\prime\prime}n_k + j\hat{\varphi}''_l\bigr). \tag{15}$$

- Calculate the DFT estimate for the $m$-th component:

$$\hat{X}_m(k) = \frac{1}{K}\sum_{k=1}^{K}\hat{x}_m(n_k)\exp\Bigl(-j\frac{2\pi k}{N}n_k\Bigr). \tag{16}$$

- Frequency estimate

$$\hat{\omega}_m = \frac{2\pi}{N}\hat{k} = \frac{2\pi}{N}\arg\max_k|\hat{X}_m(k)|\,. \tag{17}$$

  The Aboutanios-Mulgrew interpolation for this frequency estimate is performed as given below.

- Set $\delta = 0$, and for $q = 1 : Q$

$$\delta = \delta + \frac{1}{2}\frac{|\hat{X}_m(\hat{k}+\delta+\frac{1}{2})| - |\hat{X}_m(\hat{k}+\delta-\frac{1}{2})|}{|\hat{X}_m(\hat{k}+\delta+\frac{1}{2})| + |\hat{X}_m(\hat{k}+\delta-\frac{1}{2})|}\,. \tag{18}$$

- Update frequency estimate as

$$\hat{\omega}^{(m)\prime\prime} = \hat{\omega}_m + \frac{2\pi}{N}\delta\,. \tag{19}$$

- Amplitude and phase are updated as

$$\hat{A}''_m = \frac{1}{K}\Bigl|\sum_{k=1}^{K}\hat{x}_m(n_k)\exp(-j\hat{\omega}^{(m)\prime\prime}n_k)\Bigr|, \tag{20}$$

$$\hat{\varphi}''_m = \frac{1}{K}\measuredangle\sum_{k=1}^{K}\hat{x}_m(n_k)\exp\bigl(-j\hat{\omega}^{(m)\prime\prime}n_k\bigr). \tag{21}$$

This stage can be repeated several times.

## 4 Simulation study

Within the simulation study sum of sinusoids (2) is considered. The required number of samples according to the Nyquist criterion is $N = 1024$. Frequencies of sinusoids are selected randomly by the uniform distribution in the interval $\omega_i \in [-\rho\omega_{\max}, \rho\omega_{max})$ where $\omega_{\max} = \pi/\Delta$ is maximal frequency according to the Nyquist criterion, $\Delta$ is the sampling interval. To avoid aliasing effects we set $\rho = 0.99$. Phases and amplitudes are selected randomly in ranges $\varphi_i \in [0, 2\pi)$ and $A_i \in [0.5, 1]$, respectively. The minimal distance between frequencies is set to three frequency bins $6\pi/(N\Delta)$.

Experiments are performed with different number sinusoids $M \in [5, 60]$ with an increment of 5 components (5:5:60 in MATLAB notation) and the number of available samples in the range $K \in [40, 640]$. Three sets of experiments are conducted: (a) missing samples when it is assumed uniform sampling according to the Nyquist rate but with a large portion of samples unavailable; (b) previous case but for a Gaussian noise environment; (c) samples on a random position. The results of these experiments are described in three subsequent subsections.

### *4.1 Missing samples*

Figure 1 illustrates the percentage of outliers for $M =$ 5, 20, 40, and 55 sinusoids as a function of the available number of samples $K$. The blue line represents the percentage of outliers in frequency estimation after the first algorithm stage, green line after the third stage, red line after the third stage is repeated once, and the black line is for 6 re-runs. The percentage of outliers decreases with an increasing number of involved algorithms steps as can be predicted. The improvement is the most emphatic around the breakdown point of the algorithm. For $M = 55$ the breakdown point of the algorithm is about $K =$250 samples. After the first stage of the algorithm, it is required about 350 samples to eliminate outliers while

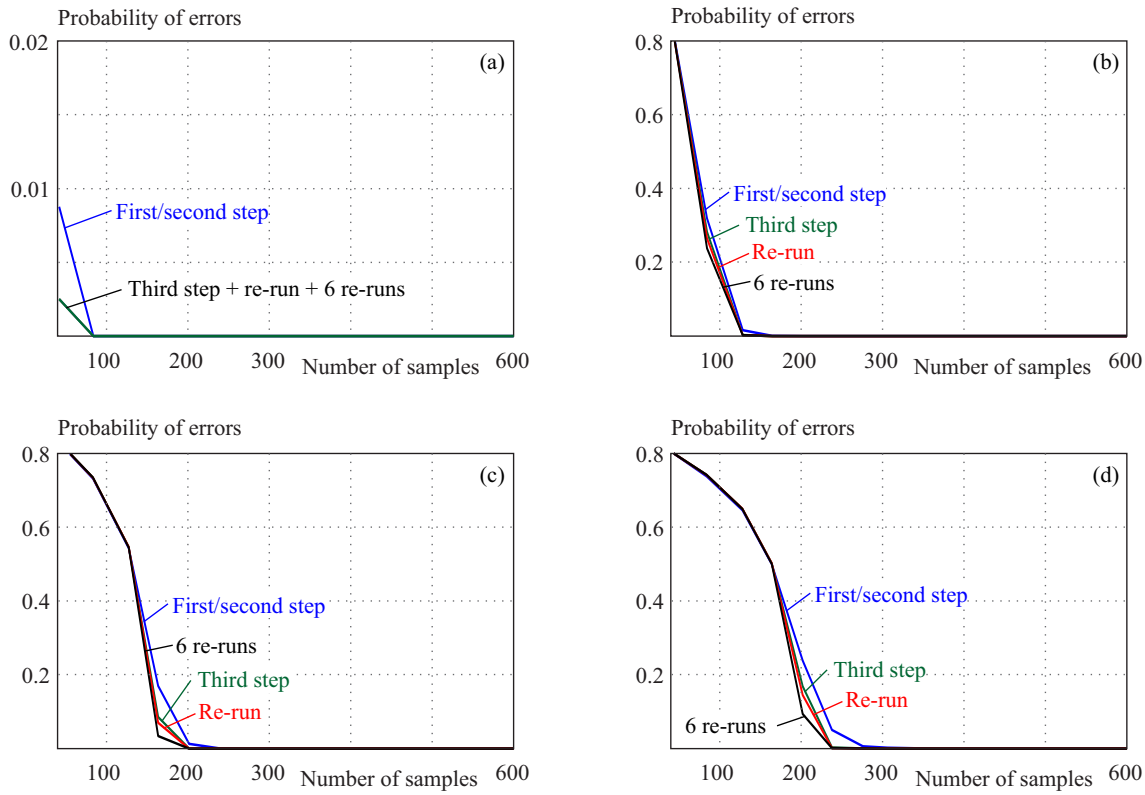


**Fig. 1.** Percentage of outliers for a various number of sinusoidal components ($M = 5,\ 20,\ 40,\ 55$) in the function of number of available random samples $K$: blue line – first stage, green line – third stage, red line – a re-run of the third stage, black line – six re-runs of the third stage

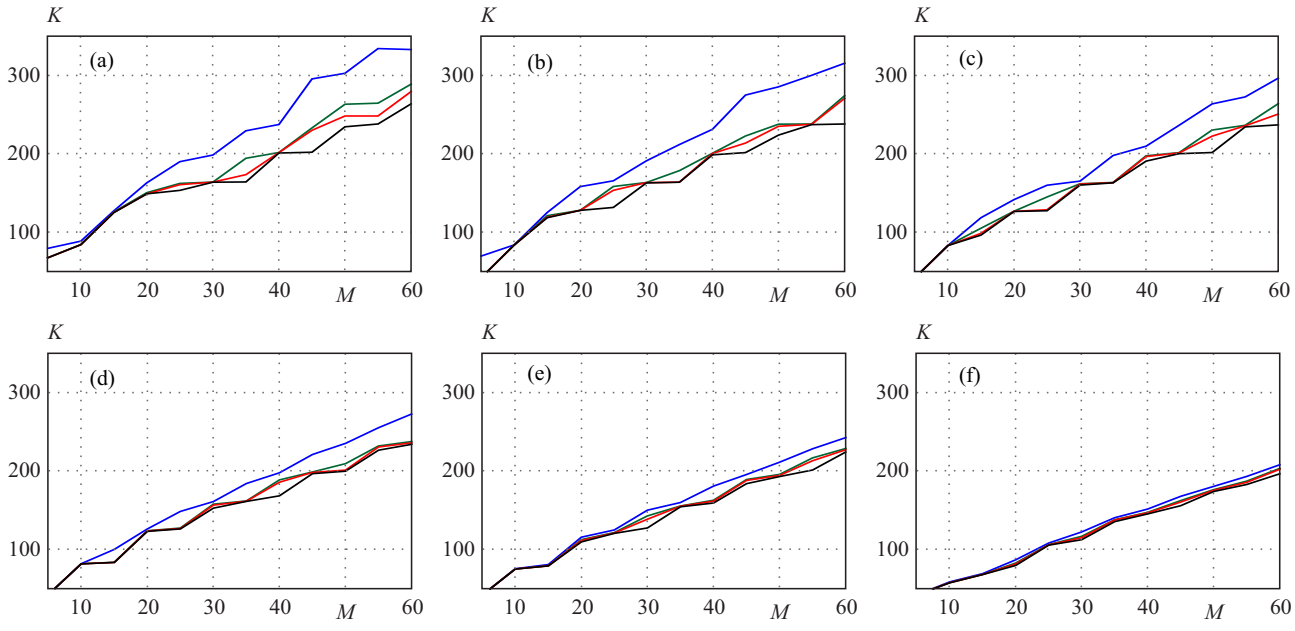


**Fig. 2.** Required number of samples for achieving percentage of outliers in frequency estimation below specific thresholds: (a) – 0.1%; (b) – 0.3%; (c) – 1%; (d) – 3%; (e) – 10%; (f) – 30%, as function of number of signal components: blue – after first step, green – after third step, red – after third step is re-run, black – after 6 re-runs of the third stage

for the algorithm with six re-runs it is required only about 240 samples, *ie*, improvement of about 30%.

For further comparison, we have given number of samples $K$ required to reduce the percentage of outliers below specific thresholds 0.1%, 0.3%, 1%, 3%, 10%, and 30% in Figure 2. It can be seen that for $M = 60$ number of outliers below 0.1% is achievable in the first stage with 340 available samples, while the algorithm with re-runs of

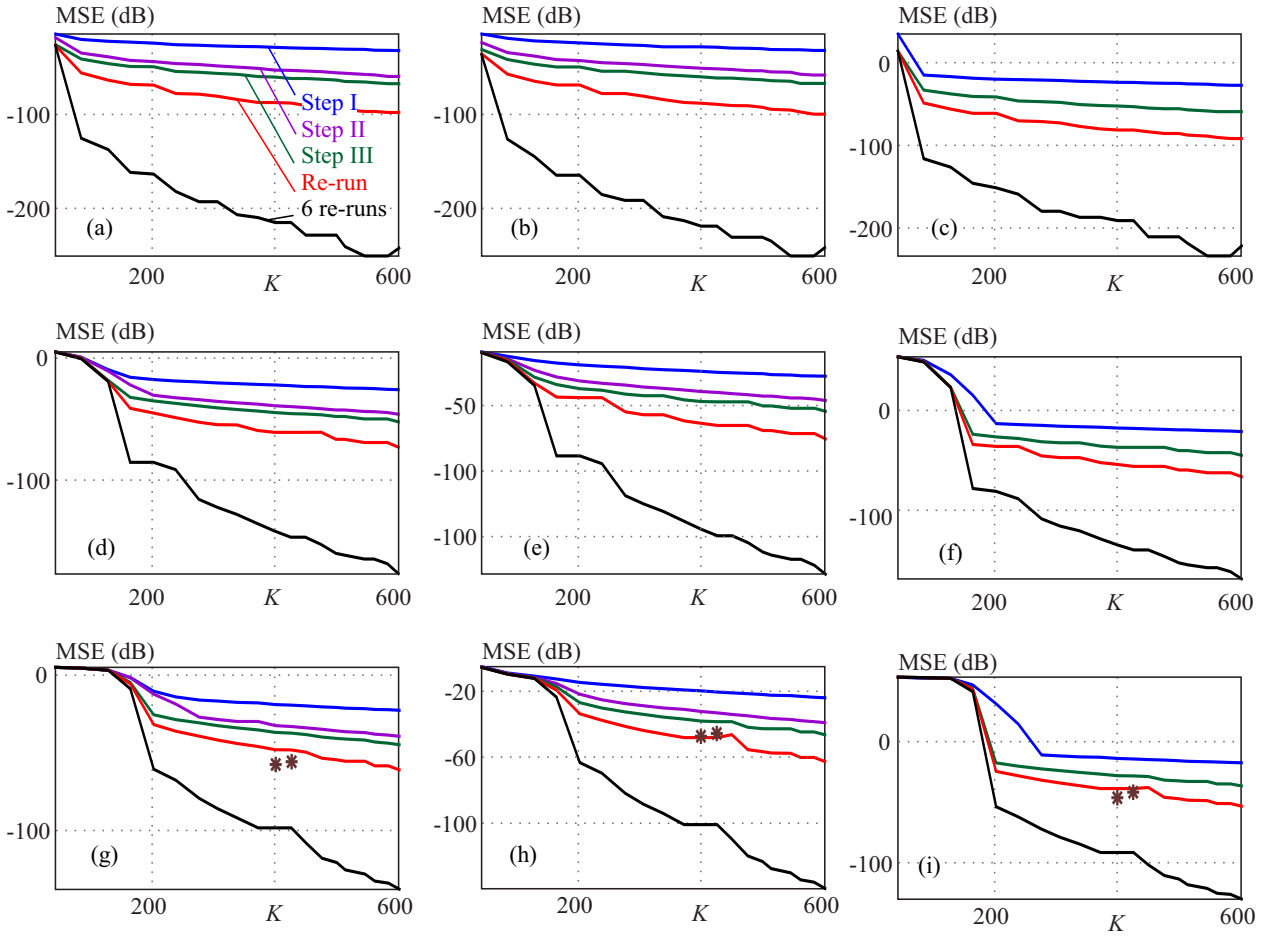


**Fig. 3.** MSE in the estimation of parameters in function of $K$: top row – $M = 5$, middle row – $M = 20$, bottom row – $M = 40$: left column – phase estimation; central column – amplitude estimation; right column – frequency estimation, blue – first stage, magenta – second stage, green – third stage, red – a re-run of the third stage, black – 6 re-runs of the third stage, * – MSE in case with under performing estimates included

the third stage requires only 260 samples. The difference is more emphatic for a larger number of signal components and a smaller threshold.

The mean squared error (MSE) in the estimation of signal phases, amplitudes, and frequencies is depicted in Figure 3 for signals with $M = 5$, 20, and 40 components obtained with 200 independent trials for each $K$ and $M$. The MSE sharply decreases above value $K$ where the number of outliers decreases toward zero. Substantial improvement is achieved with re-running of the third algorithm stage. For $M = 40$ only for two components out of 160000 ($M = 40$ components $\times 200$ trials $\times 20$ different values of $K$) obtained accuracy in parameter estimation after six re-runs of the third stage are significantly worse than for other components and trials. These two components are not taken into account for MSE evaluation, *ie*, their effect is depicted with black stars at appropriate places. Note that such estimates are not in fact outliers since the frequency estimation of this component is still relatively accurate. For one of them, the absolute error in the frequency estimation is 0.07, *ie*, far below the single frequency bin ($\Delta\omega = \pi$). There is a significant improvement in the process of re-running the third stage of the algorithm. After the first stage, all components have an error in frequency estimation larger than 0.01 and this number decreases to 22% of components after the first run of the third stage. Therefore, we think that couple of components estimated with such inaccuracy out of 160000 is acceptable after several re-runs.

For $M = 20$ and $K = 130$ we have an average of 1.6% of outliers in the first stage. Figure 4 depicts one trial with $M = 20$ and $K = 130$ where an outlier appears in frequency estimation after the first stage. Exact frequencies are given on the $x$-axis while the $y$-axis corresponds to the estimated frequencies. Estimates should appear as close as possible to the diagonal. In the considered trial we have two obvious off-diagonal outliers depicted with arrows. They are caused by the side lobe of close signal components (around $\omega = 0$ and $\omega = -1500$). We can also observe two additional components between $\omega \in [400, 800]$ clearly above the diagonal line but not too far as in the case of outliers. These two components are accurately estimated after the third stage of the algorithm while outliers required a re-run of the third stage. The top part of Figure 5 gives the square root of the absolute error in the estimation of frequencies for this experiment for each component sorted in decreasing order by amplitude. Blue bars represent errors in estimation after the

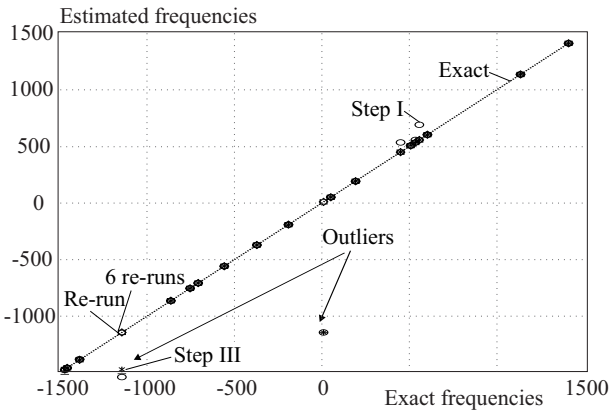


**Fig. 4.** Frequency estimates for a trial with $M = 20$ and $K = 130$, $x$-axis – the exact value of frequencies; $y$-axis – estimated frequencies, circle – first stage; star – second stage; diamond – third stage; square – 6 re-runs of the third stage

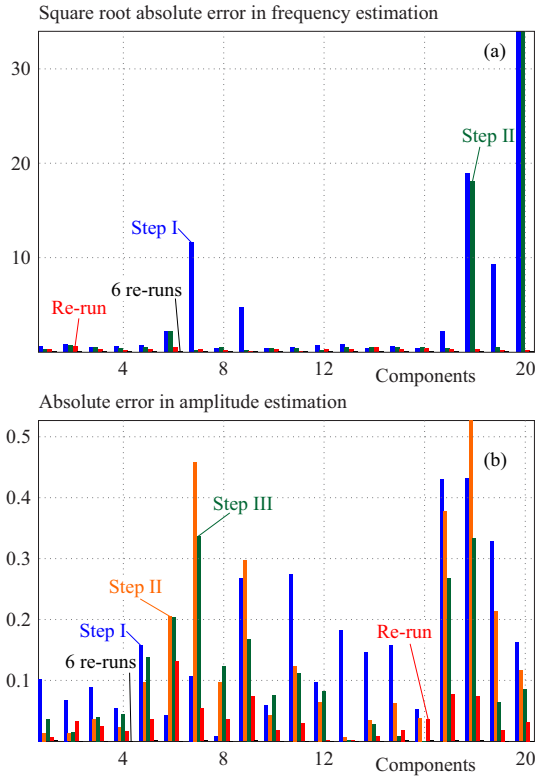


**Fig. 5.** Frequency and amplitude estimation in a trial for $M = 20$ and $K = 130$, top – square root absolute errors in frequency estimation; bottom – absolute errors in amplitude estimation, blue – first stage, magenta – second stage, green – third stage, red – after re-run of the third stage, black – 6 re-runs of the third stage

first stage with long bars on weaker components corresponding to outliers. Obviously, after the first stage error is more emphatic for weaker components as expected. They remain large even after the third algorithm stage represented with green bars. However, errors are in general significantly smaller after the third stage (green are shorter than blue bars). Red bars after the first re-run of the third stage are still visible (maximal value 0.36) while black bars obtained by six re-runs of the procedure are almost negligible (maximal value 0.056).A similar situation appears at the bottom part of Figure 5 where absolute values of errors in the estimation of amplitudes after different algorithm stages are shown. Again it can be seen a significant drop in the absolute error after re-running the third algorithm stage. After the third stage,maximal absolute error is 0.34, re-running once reduces it to 0.132, while after six re-runs maximal absolute error does not exceed 0.0009.

### *4.2 Gaussian noise environment*

The robustness of the proposed technique has been tested in the experiments with the Gaussian noise environment. We have added the Gaussian white complex noise with independent real and imaginary components and with variance $\sigma^2$. Figure 6 depicts the effect of additive noise on increasing the percentage of outliers. For brevity reasons, we have presented only results after the third algorithm stage with six re-runs. It can be observed that for both cases, $M = 20$, Figure 6(a) ,and $M = 40$ components (Figure 6(c)), we have a moderate increase in the percentage of outliers to the noiseless case. For example, for $M = 20$ and $K = 130$, the percentage of outliers increases from below 0.1% for the noiseless case to about 1.3% for $\sigma^2 = 2$. Similarly, for $M = 40$, and $K = 160$ the percentage of outliers increases for $\sigma^2 = 2$ only for 0.08% to the noiseless case. In addition, Figures 6(b) and (d) present a decrease in the percentage of outliers between the first and six re-runs of the third stage. Behavior is very similar for noisy and noiseless cases but more emphatic for the noisy case with higher values $K$ than in the case of the noiseless signal. This is an important feature since for noisy environment outliers can be expected more frequently for higher $K$.

Figure 7 gives the MSE in the estimation of phases (top row), amplitudes (middle row) and frequencies (bottom row) for $M = 5$ (left column), $M = 20$ (central column), and $M = 40$ components (right column), as a function of the noise variance $\sigma^2$ for various numbers of available samples $K$ for six re-runs of the third algorithm stage.

### *4.3 Nonuniformly subsampled signal*

Final experiments are related to random nonuniform sampling performed in the considered interval $t \in [-T/2, T/2)$ instead of random selection for the set of uniformly spaced samples. Figure 8 depicts the probability of outliers in the estimation of signal parameters for various algorithm stages and the number of signal components. Obtained results are similar to those in Figure 1 but it can be noted that here it is required approximately 25% more samples to achieve the same accuracy. The reason behind this is the higher variance in estimation caused by nonuniform sampling [9].

The MSE in the estimation of phases (top row), amplitudes (middle row), and frequencies (bottom row) for $M = 5$ (left column), $M = 20$ (central column), and $M = 40$ components (right column), for nonuniformly sampled signals, is given in Figure 9. Only for a single

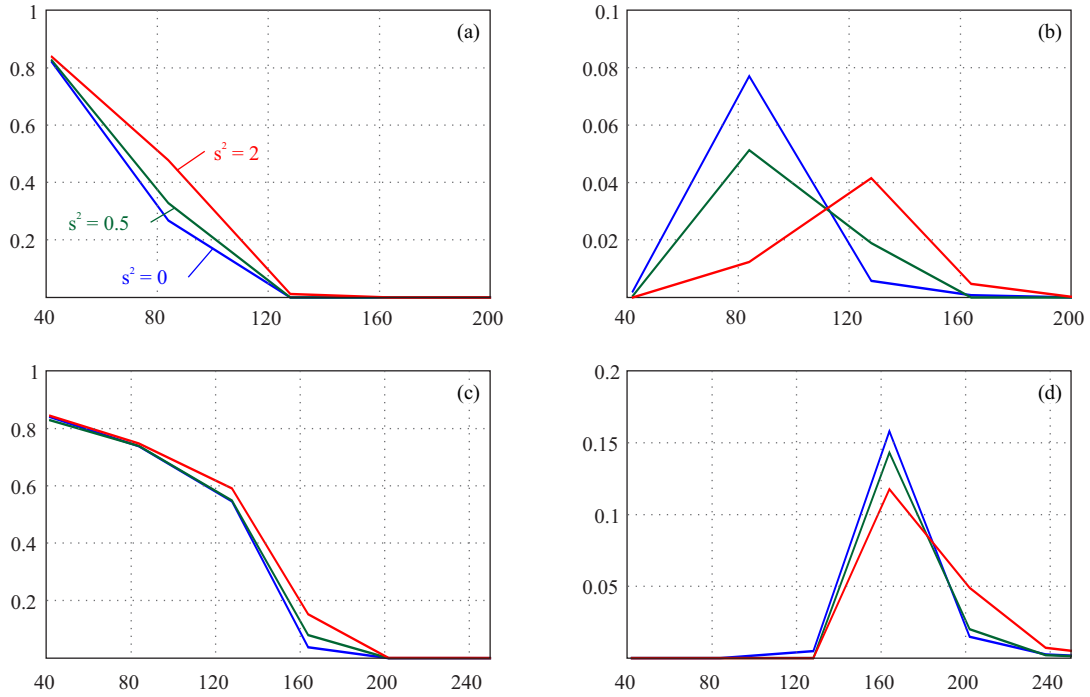


**Fig. 6.** Percentage of outliers infrequency estimation for noisy environments: (a) – after six re-runs of the third stage for $M = 20$, (b) – difference between the percentage of outliers after the first stage and after six re-runs of the third stage for $M = 20$, (c) – after six re-runs of the third stage for $M = 40$, (d) – difference between the percentage of outliers after the first stage and six-re-runs of the third stage for $M = 40$: blue line – noiseless signal $\sigma^2 = 0$, green line – $\sigma^2 = 0.5$, red line – $\sigma^2 = 2$

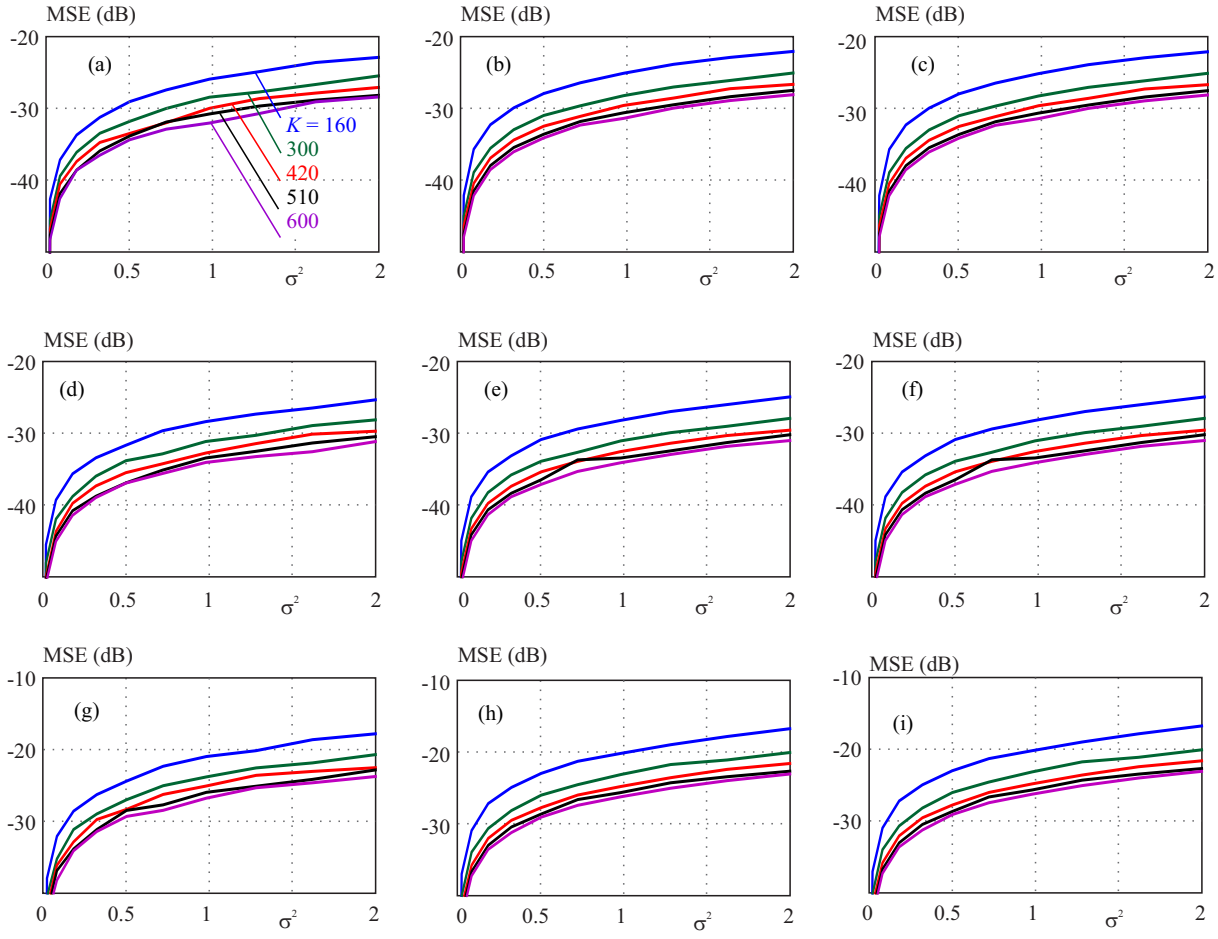


**Fig. 7.** MSE in the estimation of parameters of noisy signals in the function of $\sigma^2$, for various numbers of available samples $K$: left column – $M = 5$, middle column – $M = 20$, right column – $M = 40$, top row – phase estimation, central row – amplitude estimation, bottom row – frequency estimation

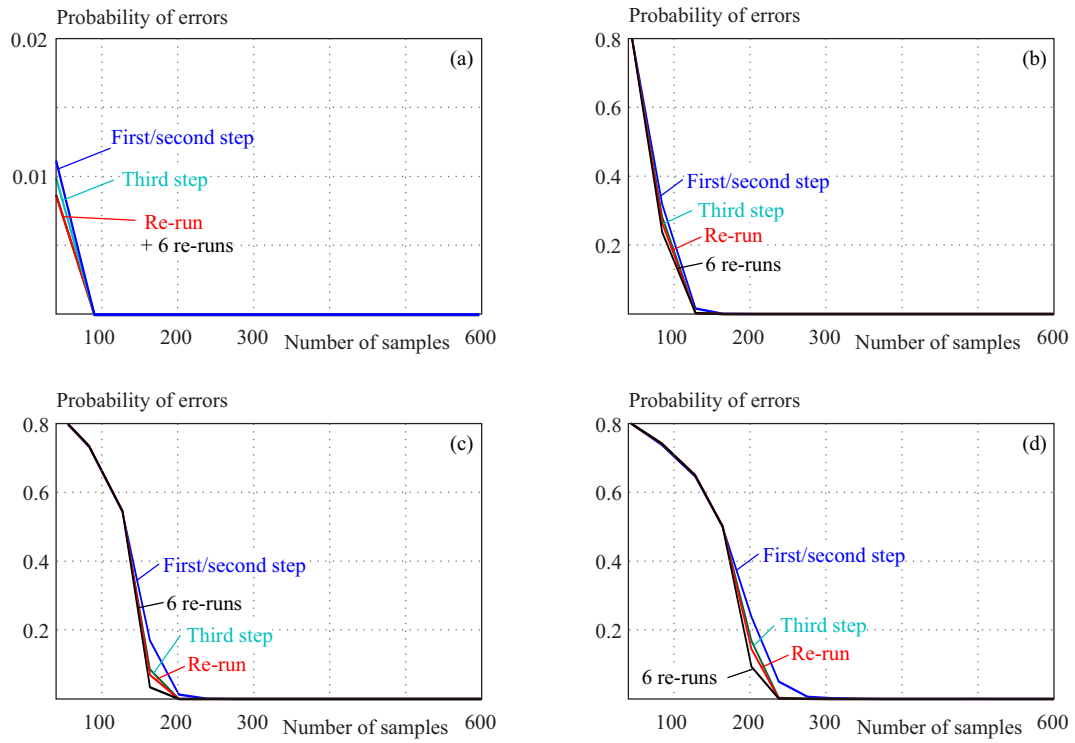


**Fig. 8.** Percentage of outliers for a various number of sinusoidal components: (a) – 5, (b) – 20, (c) – 40, and (d) – 55) as a the function of number of available random samples $K$ for signal sampled in random time instants in the given interval (nonuniform sampling): blue line – after the first stage, green line – after the second stage, red line – after re-run of the third stage, black line – six re-runs of the third stage

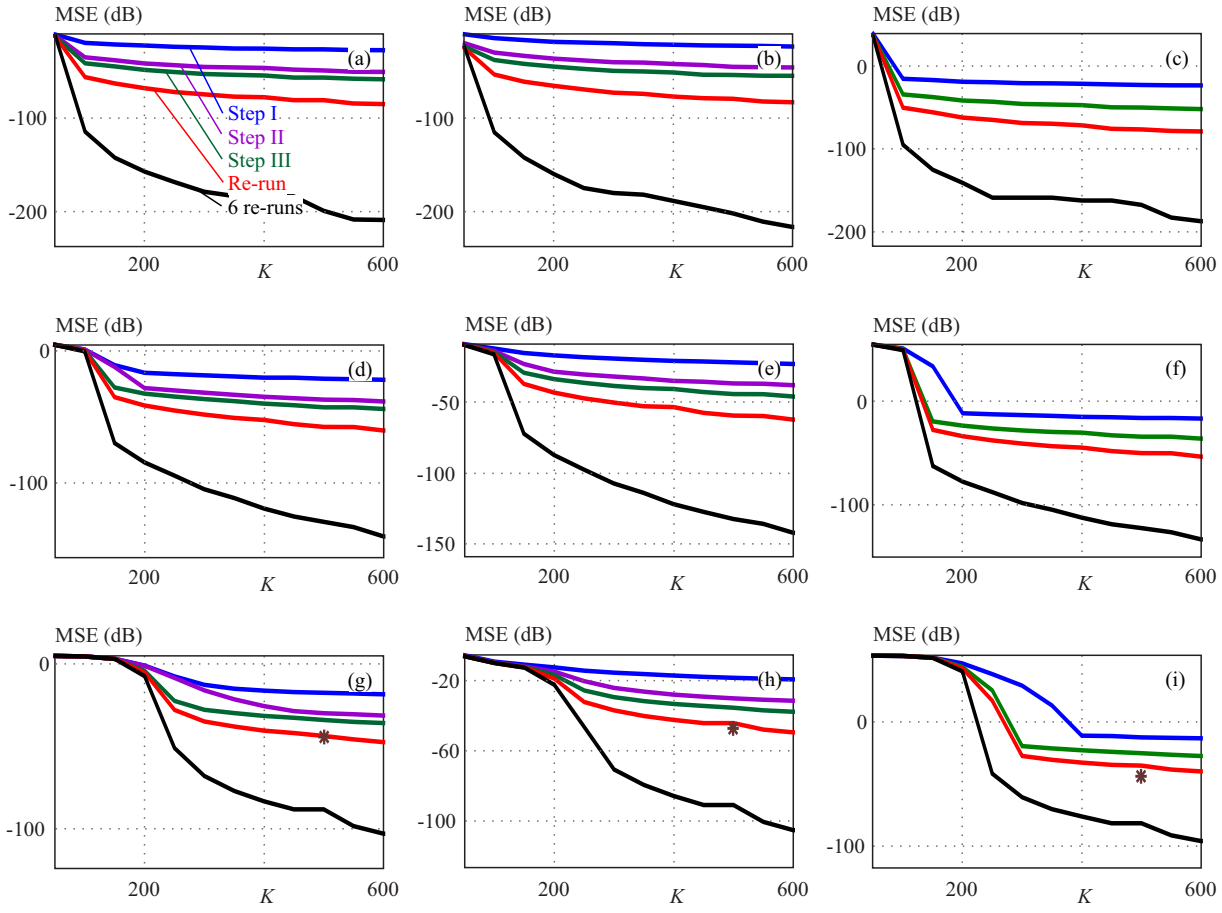


**Fig. 9.** MSE: top to bottom row with $M = 5, 20, 40$: left column – phase estimation, central column – amplitude estimation, right column – frequency estimation: blue – after the first stage, magenta – after the second stage, green – after the third stage, red – after re-run of the third stage, black – after six re-runs *MSE in the case with underperforming estimates included

component in a single trial for $M = 40$ and $K = 500$, we noted an estimate with error significantly above the other components for six re-runs of the third stage. It is excluded from the MSE plot but again black asterisk is used to denote its influence on the MSE. We refrain to call it the outlier since the estimation error for this component is only $0.09$. For $K = 500$ and $M = 40$ all components after the first stage have absolute error above $0.01$. However, after a single re-run of the third-stage 175 components (out of 8000 components, $M = 40$, and 200 trials) have an absolute error greater than $0.01$, 102 components have an absolute error greater than $0.05$, and only 3 absolute errors greater than $0.1$. After six re-runs as already stated remains a single component with an absolute error greater than $0.01$.

## 5 Conclusion

The algorithm for precise estimation of multicomponent sinusoidal signals with missing samples is proposed. It consists of three stages. The goal of the first two stages is to find components and to get at least a rough estimation of parameters while true refinement is achieved in the third stage. Each component in this stage is estimated with the assumption that the other components are removed from the mixture. The Aboutanios-Mulgrew algorithm, a simple but effective technique, has been used in the refinement process. We have performed the simulation study showing that re-running the third stage effectively improves accuracy in the estimation of components. In a future study, we will consider derivations on the accuracy of the algorithm in terms of number of components, number of available samples,number of algorithm re-runs, and estimation of parameters for unknown number of components, *etc.*

*Acknowledgemens*

This research is supported in part by the Montenegrin Academy of Sciences and Arts.

## References

[1] D. Rife and R. Boorstyn, "Single tone parameter estimation from discrete-time observations," *IEEE Transactions on Information Theory*, vol. 20, no. 5, pp. 591–598, 1974.

[2] B. G. Quinn, "Estimating frequency by interpolation using Fourier coefficients", vol. 42, no. 5, pp. 1264-1268, May 1994.

[3] C. Candan, "A method for fine resolution frequency estimation from three DFT samples," *IEEE Signal Processing Letters*, vol. 18, no. 6, pp. 351–354, 2011.

[4] E. Aboutanios and B. Mulgrew, "Iterative frequency estimation by interpolation on Fourier coefficients," *IEEE Transactions on Signal Processing*, vol. 53, no. 4, pp. 1237–1242, 2005.

[5] E. Aboutanios, "Estimation of the frequency and decay factor of a decaying exponential in noise," *IEEE Transactions on Signal Processing*, vol. 58, no. 2, pp. 501–509, 2010.

[6] I. Djurović, "Estimation of the sinusoidal signal frequency based on the marginal median DFT," *IEEE Transactions on. Signal Processing*, vol. 55, no. 5, pp. 2043–2051, 2007.

[7] I. Djurović and V. V. Lukin, "Estimation of single-tone signal parameters by using the L-DFT," *Signal Processing*, vol. 87, no. 6, pp. 1537-1544, 2007.

[8] S. Ye and E. Aboutanios, "Rapid accurate frequency estimation of multiple resolved exponentials in noise," *Signal Processing*, vol. 132, pp. 29-39, 2017.

[9] L. Stanković, M. Brajović, I. Stanković, C. Ioana, and M. Daković, "Reconstruction error in nouniformly sampled approximately sparse signals," *IEEE Geoscience and Remote Sensing Letters*, vol. 17, 2020, doi: 10.1109/LGRS.2020.2968137.

[10] L. Stanković, M. Daković, I. Stanković, and S. Vujović, "On the errors in randomly sampled nonsparse signals reconstructed with a sparsity assumption," *IEEE Geoscience and Remote Sensing Letters*, vol. 14, no. 12, pp. 2453-2456, 2017, doi: 10.1109/LGRS.2017.2768664.

[11] L. Stanković and M. Daković, "On a gradient-based algorithm for sparse signal reconstruction in the signal/measurements domain," *Mathematical Problems in Engineering*, Article ID 6212674, 2016, doi: 10.1155/2016/6212674.

[12] L. Stanković, S. Stanković, I. Orović, and Y. Zhang, "Time-frequency analysis of micro-Doppler signals based on compressive sensing," *Compressive Sensing for Urban Radar*, Ed. M. Amin, CRC-Press, 2014.

[13] E. J. Candes and T. Tao, "Decoding by linear programming," *IEEE Transactions on Information Theory*, vol. 51, no. 12, pp. 4203–4215, 2005.

[14] I. Djurović, L. Stanković, and J. F. Böhme, "Robust L-estimation based forms of signal transforms and time-frequency representations," *IEEE Transactions on Signal Processing*, vol. 51, no. 7, pp. 1753–1761, 2003.

Received 8 May 2021

**Igor Djurović** is currently professor at the Faculty of Electrical Engineering, University of Montenegro. He is member of Montenegrin Academy of Sciences and Arts from 2011. He has run numerous research projects and was director of the first Montenegrin Centre of Excellence in Bio-informatics (BIO-ICT). His current research interests include application of virtual instruments, time-frequency analysis-based methods for signal estimation and filtering, fractional Fourier transform applications, image processing, robust estimation, parametric and nonparametric estimation, spectral analysis, motion estimation, digital watermarking, wireless sensor networks, radar signal processing. In 2016 he was awarded with highest Montenegrin prize for scientific achievements.